CYT997: a novel orally active tubulin polymerization inhibitor with potent cytotoxic and vascular disrupting activity *in vitro* and *in vivo*

Christopher J. Burns,[1] Emmanuelle Fantino,[1] Ian D. Phillips,[1] Stephen Su,[1] Michael F. Harte,[1] Patricia E. Bukczynska,[1] Mark Frazzetto,[1] Max Joffe,[1] Irma Kruszelnicki,[1] Bing Wang,[1] Yue Wang,[1] Neil Wilson,[1] Rodney J. Dilley,[2] Soo S. Wan,[1] Susan A. Charman,[3] David M. Shackleford,[3] Rosa Fida,[3] Cathy Malcontenti-Wilson,[4] and Andrew F. Wilks[1]

[1]Cytopia Research Pty. Ltd., Richmond, [2]Bernard O'Brien Institute of Microsurgery, Fitzroy, [3]Centre for Drug Candidate Optimisation, Monash Institute of Pharmaceutical Sciences, Monash University, Parkville, and [4]The University of Melbourne Department of Surgery, Austin Health, Heidelberg, Victoria, Australia

Abstract

CYT997 is a wholly synthetic compound that possesses highly potent cytotoxic activity *in vitro* through inhibition of microtubule polymerization. CYT997 blocks the cell cycle at the G_2-M boundary, and Western blot analysis indicates an increase in phosphorylated Bcl-2, along with increased expression of cyclin B1. Caspase-3 activation is also observed in cells treated with CYT997 along with the generation of poly(ADP-ribose) polymerase. The compound possesses favorable pharmacokinetic properties, is orally bioavailable, and is efficacious per os in a range of *in vivo* cancer models, including some refractory to paclitaxel treatment. CYT997 exhibits vascular disrupting activity as measured *in vitro* by effects on the permeability of human umbilical vein endothelial cell monolayers, and *in vivo* by effects on tumor blood flow. CYT997 possesses a useful combination of pharmacologic and pharmacokinetic properties and has considerable potential as a novel anticancer agent. [Mol Cancer Ther 2009;8 (11):3036–45]

Received 2/4/09; revised 9/4/09; accepted 9/8/09; published OnlineFirst 11/3/09.

Grant support: Centre for Drug Candidate Optimisation, University of Melbourne Department of Surgery (C. Malcontenti-Wilson).

The costs of publication of this article were defrayed in part by the payment of page charges. This article must therefore be hereby marked *advertisement* in accordance with 18 U.S.C. Section 1734 solely to indicate this fact.

Requests for reprints: Christopher J. Burns, Cytopia Research Pty. Ltd., 576 Swan Street, Richmond, Victoria 3121, Australia. Phone: 61-3920-84235; Fax: 61-3920-84299. E-mail: chris.burns@cytopia.com.au

doi:10.1158/1535-7163.MCT-09-0076

Introduction

Microtubules play an essential role in cell division, intracellular transport, and motility. Several clinically important anticancer drugs such as paclitaxel and the *Vinca* alkaloids, vincristine and vinblastine (1–3), bind to microtubules thereby altering normal microtubule dynamics (4), which in turn, causes cells to arrest at the G_2-M boundary of the cell cycle and ultimately leads to apoptotic or nonapoptotic cell death (5).

Although microtubule binding agents such as the taxanes and the *Vinca* alkaloids are frontline treatments for breast, ovarian, and hormone-refractory prostate cancer, they have substantial drawbacks, notably development of resistance over time (6), the need for intravenous administration and, in the case of paclitaxel, formulation in the lipid-based solvent Chremophor EL, which itself can cause hypersensitivity and neuropathy (7). In recent years, there has been considerable research toward the identification of new tubulin-binding compounds that address the shortcomings of the classic agents (8, 9). Thus, various analogues of the taxanes and *Vinca* alkaloid classes have been reported (10, 11), as have a range of other natural product-derived compounds, such as the epothilones (12). Several small molecule tubulin-binding drugs, chemically distinct from the *Vinca* and taxanes class, have also been described. These compounds generally possess improved physicochemical and pharmacokinetic properties compared with paclitaxel and the *Vinca* alkaloids, although few possess oral activity. Whereas the clinical efficacy of some of these new agents has been mixed, it has become apparent that several of these small molecule microtubule-binding agents exhibit disruptive effects on the tumor vasculature at concentrations well below their maximum tolerated dose (13). We describe herein CYT997, a microtubule-disrupting agent that possesses potent cytotoxic activity *in vitro*, an attractive pharmacokinetic profile, oral activity in two separate xenograft models, and in addition, a clear indication of antivascular effects *in vitro* and *in vivo*.

Materials and Methods

CYT997 was prepared as previously described (14). Paclitaxel, colchicine, vincristine, and vinblastine were purchased from Sigma. Animal studies were conducted in accordance with the Australian and New Zealand Council for the Care of Animals in Research and Training Guidelines and with the approval of the institutional animal experimentation ethics committees.

Cell Culture

A broad selection of cancer cell lines (see Table 1) obtained from the American Type Culture Collection was selected and

Table 1. IC_{50} (nmol/L) for CYT997 on a range of cancer cell lines, as determined by cell viability assays

DU145	A549	Ramos	KHOS/NP	A375	HCT-15	HT1376	BT-20
73	21	80	101	49	52	93	58
A431	PA-1	U937	HepG2	TF-1	Baf3/TelJAK2	PC3	K562
51	48	21	9	32	23	27	20

NOTE: Cell lines are DU145, human prostate carcinoma; A549, human lung carcinoma; Ramos, human Burkitt's lymphoma; KHOS/NP, human osteosarcoma; A375, human melanoma; HCT-15, human colon carcinoma; HT1376, human bladder carcinoma; BT-20, human breast carcinoma; A431, human epithelial carcinoma; PA-1, human ovarian teratocarcinoma; U937, human leukemic monocyte lymphoma; HepG2, human hepatocellular liver carcinoma; TF-1, human erythroleukemia; BaF3/TelJAK2, constitutively active JAK2; PC-3, human prostate carcinoma; K562, human chronic myelogenous leukemia.

cultured essentially according to its guidelines. Baf3/TEL JAK2 cells were established as described in ref. (15). TEL-induced oligomerization of the TEL-JAK2 fusion protein results in the constitutive activation of JAK2 tyrosine kinase activity, conferring cytokine-independent proliferation to the interleukin 3–dependent Ba/F3 hematopoietic cell line. This activating JAK2 fusion has been identified in chromosomal translocations found in atypical chronic myelogenous leukemia and pre–B-cell acute lymphoblastic leukemia (16).

Cell Proliferation Assay

Cell proliferation was assessed (IC_{50}, nmol/L) with either the Alamar blue or MTT assays after exposure to vehicle (0.1% DMSO) or CYT997 for 72 h. Cells were cultured in flat-bottomed 96-well plates at predetermined optimal densities and exposed to DMSO vehicle (0.1% final concentration) or varying concentrations of CYT997 for 72 h at 37°C. For MTT assays, 5 mg/mL of MTT was added to all wells, plates were incubated for 6 h at 37°C, and then lysis buffer was added (10% SDS in 0.01 N HCl) and absorbance was measured at 620 nm in a BMG Technologies Lumistar or Polarstar plate reader. For Alamar blue assays, Alamar blue (10 μL/well, AbD Serotec) was added to each well and the plates were incubated at 37°C for 4 h. The fluorescence was then measured using a fluorescence plate reader (BMG Technologies Polarstar) with an excitation filter at 544 nm and an emission filter at 590 nm.

Fluorescence-Activated Cell Sorting Studies

Cell Cycle Analysis. Following incubation of A431 cells with 1 μmol/L of CYT997 or DMSO vehicle for specified time periods, cells were fixed and permeabilized with 70% ethanol in PBS and incubated at 4°C overnight. RNase-treated samples (10 μg RNase/mL for 20 min at 37°C) were stained with propidium iodide (5 μg/mL) at 4°C for a minimum of 10 min. Cell cycle variables were determined by fluorescence-activated cell sorting (FACS) analysis using a Beckman-Coulter Quanta SC MPL system and analyzed using CXP Software.

Apoptosis Analysis. A549 cells (human epithelial lung cancer) were plated and allowed to adhere overnight before treating with CYT997 (250 nmol/L) or vehicle. At the specified time points, cells were detached and collected. Annexin staining was done using the Vybrant Apoptosis Assay Kit no. 2 from Invitrogen, using Alexa 488 Annexin V and propidium iodide, following the protocol of the manufacturer. Cells were stored on ice and analyzed on a Beckman Coulter Quanta MPL within 1 h of preparation. Annexin V–positive cells were determined using two-channel analysis.

Tubulin Polymerization Assay

Turbidimetric assays of microtubule assembly were done by incubating bovine microtubule protein in cuvettes at 37°C in a thermostatically controlled spectrophotometer (BMG Technologies Polarstar) measuring the change in absorbance at 340 nm over time in PEM buffer [80 nmol/L PIPES (pH 6.9), 2 mmol/L $MgCl_2$, 0.5 mmol/L EGTA, and 5% glycerol]. Compounds were added to 100 μL of tubulin/GTP/glycerol to a final concentration of 250 nmol/L, 5 or 10 μmol/L (CYT997), or 2 μmol/L (colchicine).

Fluorescence Immunocytochemistry

A549 cells were plated sparsely in an eight-well chambered cover glass (Lab-Tek) and allowed to adhere overnight before treating with CYT997 and cultured further for up to 24 h. At the end of treatment, cells were fixed in cold methanol, pretreated with protein block solution (Dako), and incubated with monoclonal anti–bovine-α tubulin (Sigma) overnight, washed in PBS and incubated with Alexa Fluor 488 goat anti-mouse IgG (H+L; Invitrogen) for 30 min. Cells were washed in PBS and micro-tubule distribution imaged on either an Olympus IX81 fluorescence microscope or Bio-Rad MRC1024 confocal microscope. Propidium iodide was added at 5 μg/mL to stain for nuclei.

Human Umbilical Vein Endothelial Cell Monolayer Permeability Assay

Human umbilical vein endothelial cell (HUVEC) cells were obtained from Invitrogen and cultured in Media 200 supplemented with low serum growth supplement. The *In vitro* Vascular Permeability Assay Kit was purchased from Chemicon.

HUVEC cells were trypsinized, collected, and seeded onto collagen-coated inserts at 200,000 cells per insert and cultured for 72 h at 37°C to form a monolayer. The cells were then treated with the increasing concentrations of CYT997, CA4P, or vehicle (0.1% DMSO) for various amounts of time (1, 2, 4, and 24 h). After treatment, media with compound was removed from inserts, which were then moved to a fresh collection plate containing 500 μL of medium per well. FITC-Dextran (150 μL, prepared at 1:4,000 dilution with medium) was added on top of the cells. Cell monolayers were incubated with FITC-Dextran for 5 min at room temperature, allowing it to permeate through the cell monolayer. The extent of permeability was determined by measuring

the fluorescence of the plate well solution using a fluorometer with a 485 and 530 nm filter set. Monolayers were also treated with growth medium only and inserts were also tested without cell monolayer.

Western Blot Analysis

PC3 cells (human prostate cancer) or A549 cells were subcultured in complete medium in T75 flasks at 37°C, 5% CO_2 overnight before serum starvation. Following 48 h of serum starvation, 1 μmol/L of CYT997 or vinblastine was added, followed by the addition of serum to 10% v/v. Cell were harvested, centrifuged, and washed with PBS at the time points indicated after compound treatment. Cell pellets were lysed by adding CHAPS extract buffer [50 mmol/L PIPES/NaOH (pH 6.5), 2 mmol/L EDTA, 0.1% CHAPS, 5 mmol/L DTT, 20 μg/mL leupeptin, 10 μg/mL pepstatin, 10 μg/mL aprotinin, and 1 mmol/L phenylmethylsulfonyl fluoride]. Protein (50 μg) from cleared lysates was loaded on SDS-PAGE and analyzed by Western blot with antibodies: cleaved caspase-3 (Asp175), cleaved caspase-9 (Asp330), and cleaved poly(ADP-ribose) polymerase (PARP; Asp214; Cell Signaling Technology).

Cell pellets of A549 cells were lysed in radioimmunoprecipitation assay buffer [50 mmol/L Tris-HCl (pH 7.4), 150 mmol/L NaCl, 2 mmol/L EDTA, 1% NP40, 0.1% SDS] and 50 μg of protein from cleared lysates loaded on SDS-PAGE gels. Western blot analysis was done with antibodies against cyclin B1 (V152), pSer70-Bcl2, and pSer63-c-*Jun* (Cell Signaling Technology).

Pharmacokinetic Analysis

On the day prior to dosing, a cannula was surgically inserted into the left carotid artery of male Sprague-Dawley rats (~300 g) and also into the right jugular vein for rats that would receive CYT997 via the intravenous route. Cannulae were exteriorized by tunnelling subcutaneously to emerge above the scapulae. Fasted rats were dosed with CYT997 at a nominal dose of 5 mg/kg i.v. (in either pH 4 acetate buffer with 5% propylene glycol or 0.1 mol/L captisol; Cydex Pharmaceuticals, Inc.) or 25 mg/kg p.o. (as the mesylate salt in water). Food was reinstated at 4 h postdosing. Plasma samples were collected over 24 h and stored at −20°C for a maximum of 2 wk prior to analysis. Plasma samples and calibration standards were processed by precipitating the proteins with acetonitrile, and the supernatant obtained by centrifugation was analyzed by liquid chromatography-mass spectrometry using a Micromass Quattro Ultima Pt triple quadrupole instrument coupled with a Waters 2795 high-performance liquid chromatography instrument.

In vivo Tumor Models

PC3 Xenograft Model. Human PC-3 cells (10^6) were inoculated s.c. in the right ventral flank of male nude mice. Subcutaneous tumor sizes were measured from day 8 postinoculation of cells, and mice were allocated at random to treatment groups on day 12. Administration of compounds (CYT997: 7.5, 15, or 30 mg/kg/d by oral gavage thrice a day; paclitaxel: 10 mg/kg i.v., thrice a week) or vehicle (NMP/PEG300/saline) commenced 13 d postinoculation of PC3 cells (treatment day 1). Dosing at 30 mg/kg/d was stopped after 11 treatment days due to excessive weight loss (>10%), and resumed after 7 d at 25 mg/kg/d for the remainder of the experiment (3 treatment days). The dimensions of subcutaneous PC3 tumors were measured thrice per week on alternate weekdays, and the experiment was ended on treatment day 21, when the tumors in control untreated mice reached 2 cm^3.

4T1 Syngeneic Model. Female BALB/c mice were inoculated with 10^6 murine 4T1 breast cancer cells in the mammary fat pad. Tumor sizes were measured from 7 d postsurgery, and mice were allocated at random to treatment groups (n = 10/group) after 11 d. Mice were given CYT997-free base (7.5, 15, 30 mg/kg/d) by oral gavage (10 mL/kg), thrice a day CYT997 was formulated in NMP/PEG300/saline; the vehicle control group received NMP/PEG300/saline (10 mL/kg, thrice a day). Paclitaxel (10 mg/kg i.v. thrice a week) or platinol (7.5 mg/kg, weekly i.v.) were given to two positive control groups. Dosing at 30 mg/kg/d was stopped after 5 treatment days and resumed on treatment day 10 at 25 mg/kg/d for the remainder of the experiment. Tumor dimensions were measured on alternate weekdays until treatment day 13, when tumor sizes in the untreated control group reached 2 cm^3.

In vivo Laser Doppler Blood Flow Analysis

The colon cancer liver metastases model was used as previously described (17). Male CBA mice were inoculated intrasplenically with 5×10^4 mouse DMH colon cancer cells followed by splenectomy. A single dose of CYT997 (7.5 mg/kg) in 0.1 mol/L of captisol or combretastatin A4 phosphate in saline (CA4P, 100 mg/kg), or 0.1 mol/L of captisol (vehicle control) was given i.p. 20 d after inoculation of

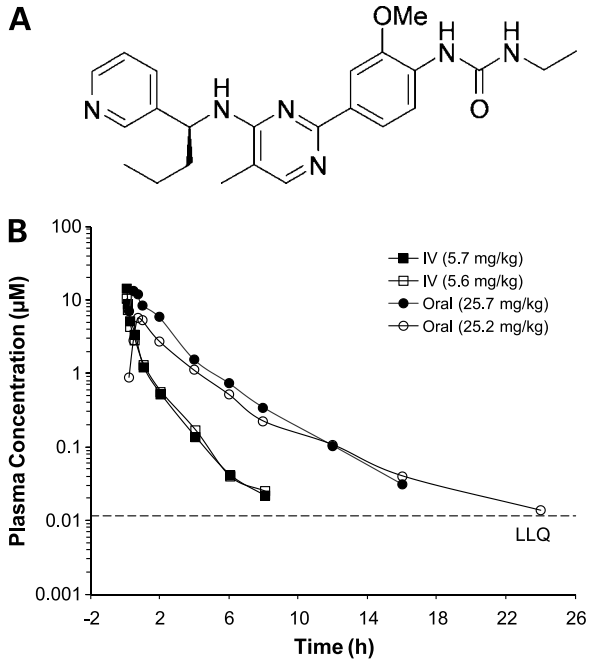

Figure 1. **A,** chemical structure of CYT997. **B,** plasma concentration versus time profiles of CYT997 after i.v. (5 mg/kg) and p.o. (25 mg/kg) dosing to fasted male Sprague-Dawley rats.

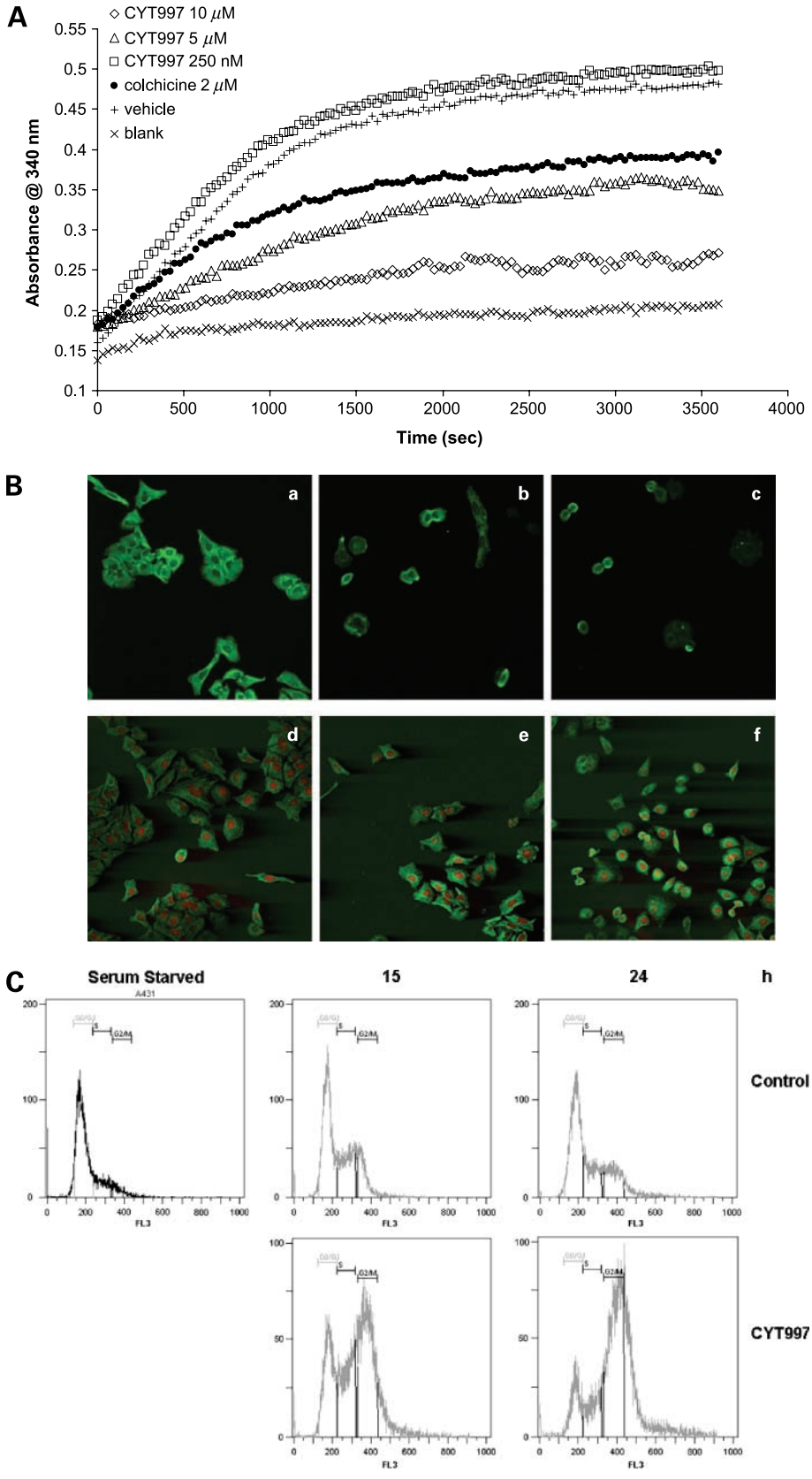

Figure 2. CYT997 exhibits a mechanism of action consistent with microtubule disruption. **A,** CYT997 inhibits the polymerization of tubulin *in vitro*. The effect of CYT997 on microtubule polymerization was determined using a conventional turbidimetric assay using bovine neuronal tubulin in which the assembly of microtubules is monitored by an increase in absorbance at 340 nm. Tubulin polymerization at 37°C in the presence of glycerol is more effectively inhibited as CYT997 concentration is increased. As a positive control, colchicine (2 μmol/L) shows partial inhibition under these conditions. From these data, we estimate the IC_{50} for inhibition by CYT997 of assembly of bovine neuronal tubulin to be 3 μmol/L. **B,** interphase α-tubulin immunostaining of A549 cells treated with CYT997 (1 μmol/L). Compared with the untreated cells (**a**), CYT997 treatment for 1 h (**b**) reduced cytoplasmic immunostaining, and in many cells, α-tubulin (*green*) seemed to redistribute to intensely labeled plaques in the peripheral cytoplasm. After 24 h continuous treatment (**c**), tubulin levels were decreased and the microtubule network was profoundly disturbed and there was evidence for cell rounding and loss of cell attachment. **d** and **e,** cells stained with α-tubulin antibody (*green*) and with nuclei stained with propidium iodide (*red*). After treatment with vehicle (**d**) or CYT997 (**e**) for 1 h, with 1 h recovery after washout, cells appear normal. **f,** cells after 1 h of treatment with CYT997 and 24 h of recovery after washout, again showing normal distribution of tubulin. **C,** effects of CYT997 on the cell cycle distribution of A431 cells. Flow cytometry studies were undertaken on fixed, propidium iodide–stained A431 cells after exposure to CYT997. Cells were serum-starved for 48 h, released from starvation for 6 h, and then CYT997 was added (1 μmol/L) for periods of 15 or 24 h. Vehicle-treated cells were tested at 15 and 24 h. Cells fixed immediately following release from serum starvation are shown for reference.

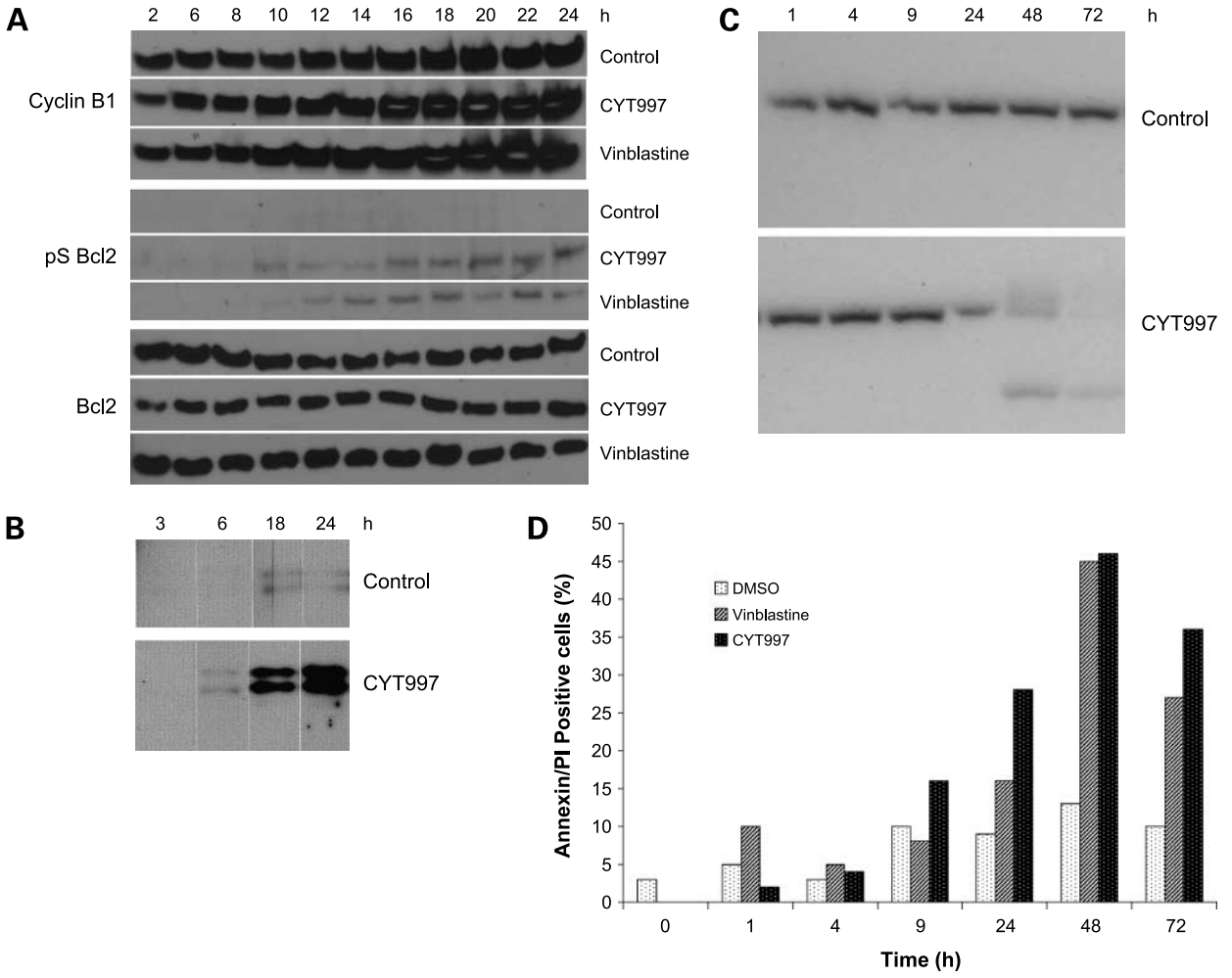

Figure 3. Exposure of cells to CYT997 causes apoptosis. **A,** CYT997 increases the expression level of cyclin B1 and the serine phosphorylation of Bcl2 but does not affect total Bcl2. Western blot analysis of control, vinblastine (1 μmol/L), and CYT997 (1 μmol/L) treated A549 cells were performed with monoclonal antibodies against cyclin B1 (V152), pSer70-Bcl2, and Bcl2. **B,** CYT997 activates the caspase pathway in PC3 cells. CYT997 activated caspase-3 in a time-dependent fashion beginning 6 h after the addition of the compound. Total extracts from PC-3 cells treated with 1 μmol/L CYT997 for the indicated times were analyzed by Western blotting using antibody to cleaved caspase-3 (Asp175) that detects the large fragment (17/19 kDa) of activated caspase-3 resulting from cleavage adjacent to Asp175. **C,** CYT997 activates the caspase pathway in A549 cells to generate PARP. PARP cleavage is observed in a time-dependent fashion beginning 6 h after the addition of the compound. Total extracts from A549 cells treated with 1 μmol/L of CYT997 for the indicated times were analyzed by Western blotting using antibody to cleaved PARP (Asp214) that detects endogenous levels of the large fragment (85 kDa) of human PARP1 produced by caspase cleavage. **D,** CYT997 increases the percentage of phosphatidylserine on the cell surface indicating apoptosis. A549 cells treated with CYT997 (250 nmol/L) or vinblastine (250 nmol/L) for the specified time periods were stained with labeled Annexin V antibody and measured by FACS.

tumor cells when established tumors were present (n = 10 and 14 mice for controls and compound-treated groups, respectively). Using an OxyFlo Multi-channel laser Doppler tissue blood flow monitor (Oxford Optronix), blood flow was measured in individual tumors (two to five tumors per liver) and adjacent liver on the liver surface of anesthetized mice, 1 or 6 h after compound or vehicle administration. Tumor blood flow was expressed as a percentage relative to normal liver blood flow.

Results

CYT997 Exhibits Broad Cytotoxicity *In vitro*

CYT997 (Fig. 1A) was derived from a lead obtained in a large-scale cell-based antiproliferation screen of small synthetic drug-like molecules. The lead was optimized for cytotoxic potency and drug-like properties, and ultimately, CYT997 was chosen for formal preclinical development (14).

CYT997 was tested against a panel of 16 cancer cell lines and the effect on cellular proliferation was determined by standard tetrazolium (MTT) or Alamar blue assays. The IC_{50} values varied from 10 to 100 nmol/L (Table 1), and no definitive trend towards particular sensitivity was exhibited by one cancer cell type over another. The potent activity of CYT997 against HCT15 cells, known to possess the multidrug resistance mechanism Pgp (MDR^+; ref. 18) indicates that the cytotoxicity of the compound is not overly affected by the presence of this efflux pump.

CYT997 Is an Orally Bioavailable Synthetic Drug-Like Molecule

Figure 1B shows the plasma concentration versus time profiles of CYT997 following intravenous and oral administration to rats. The half-life for oral administration (2.5 hours) was somewhat longer than that for intravenous administration (1.5 hours), with the absolute oral bioavailability being 50% to 70%. Similar bioavailability has been observed in the dog (data not shown). Based on these findings, we anticipated that therapeutic levels of CYT997 could be maintained in the rodent from single intravenous or oral dosing for 6 to 10 hours.

CYT997 Inhibits Tubulin Polymerization *In vitro* and Disrupts Microtubules in Intact Cells

CYT997 prevented the *in vitro* polymerization of tubulin with an IC_{50} of ~3 μmol/L (compared with the half-maximal inhibitory concentration of 2 μmol/L for colchicine under identical conditions) as determined using the conventional turbidimetric assay for tubulin polymerization (Fig. 2A). CYT997 was also capable of reversibly disrupting the microtubule network in cells, visualized using fluorescence microscopy (Fig. 2B). Thus, treatment of A549 cells with CYT997 (1 μmol/L) lead to the rapid reorganization of microtubules, including the destruction of the existing microtubule network and accumulation of tubulin in plaques within the cytoplasm of some cells. After 24 hours, major alterations in cell morphology were evident, including loss of adhesion and cell rounding. The effect of 1 hour of treatment with CYT997 was reversible and cells rapidly recovered their normal microtubule architecture. Taken together, the data indicates that CYT997 belongs to the class of anticancer agents that disrupt, rather than stabilize, tubulin-containing structures.

Cell Cycle Arrest and Induction of Apoptosis

It is well documented that compounds that inhibit tubulin polymerization cause cells to arrest at the G_2-M boundary of the cell cycle (5). The effect of CYT997 on the progression of synchronized A431 cells through the cell cycle was examined by FACS using propidium iodide staining (Fig. 2C). Although vehicle-treated cells show 15% and 19% in G_2-M phase at 15 and 24 hours (respectively), cells treated with CYT997 (1 μmol/L) had 38% and 43% of cells in G_2-M at the same time points. Furthermore, at 24 hours post-CYT997 treatment, only 66% of total cells were in the G_1, S, and G_2-M phases, which suggests that cells blocked at the G_2-M boundary do not exit back to G_1, as in the normal cell cycle, but most likely are driven towards apoptosis and

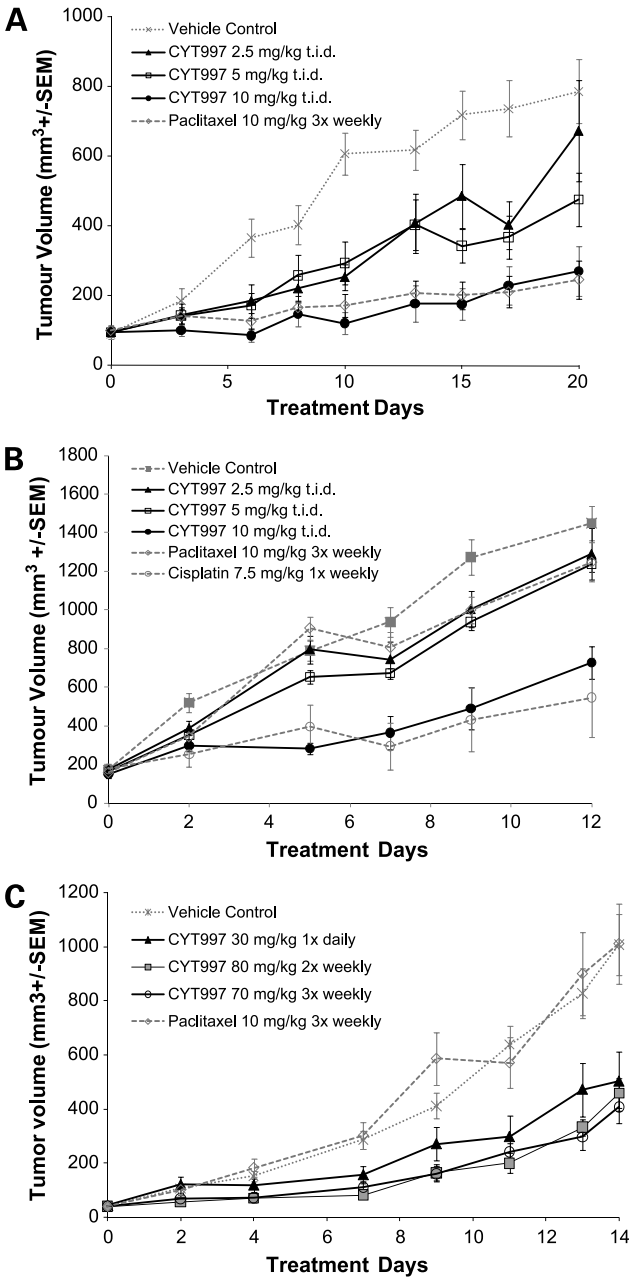

Figure 4. CYT997 is efficacious in tumor xenografts when dosed orally. **A,** volume (mean ± SEM) of subcutaneous PC3 prostate tumors in mice treated with or without CYT997 given p.o., or paclitaxel given i.v. Prostate cancer cells were inoculated s.c. in the right ventral flank of male nude mice. Subcutaneous tumor sizes were measured from day 8 postinoculation of cells, and mice were allocated at random to treatment groups (n = 10/group) day 12. Administration of compounds (CYT997: 7.5, 15, 25–30 mg/kg/d by oral gavage thrice daily; paclitaxel, 10 mg/kg i.v., thrice a week) or vehicle commenced 13 d postinoculation of cells (treatment day 1). The dimensions of subcutaneous PC-3 tumors were measured thrice a week on alternate weekdays. **B,** volume (mean ± SEM) of orthotopic 4T1 breast tumors in mice treated with or without orally administered CYT997, or i.v. paclitaxel or platinol over a 13-d treatment period. Mouse 4T1 breast tumor cells were inoculated orthotopically into the mammary fat pad of female BALB/C mice. Treatment with compounds (CYT997, paclitaxel, or platinol) or vehicle started on day 12 postsurgery (treatment day 1). Mice were given a CYT997-free base (7.5, 15, 25–30 mg/kg/d) by oral gavage (10 mL/kg) thrice a day. The untreated control group received vehicle (10 mL/kg, thrice a day). Paclitaxel (10 mg/kg, i.v. thrice a week) or platinol (7.5 mg/kg, i.v. weekly) were administered to two positive control groups. Tumor volume was measured thrice weekly. **C,** volume (mean ± SEM) of orthotopic 4T1 breast tumors in mice treated with or without orally administered CYT997 or i.v. paclitaxel over a 13-d treatment period. Four groups of 10 female BALB/c mice received doses of CYT997, and two control groups of 10 female BALB/c mice received doses of water or paclitaxel at the concentrations shown, to animals inoculated with 4T1 tumor cells on day −8 and treatment to all groups commenced on day 0.

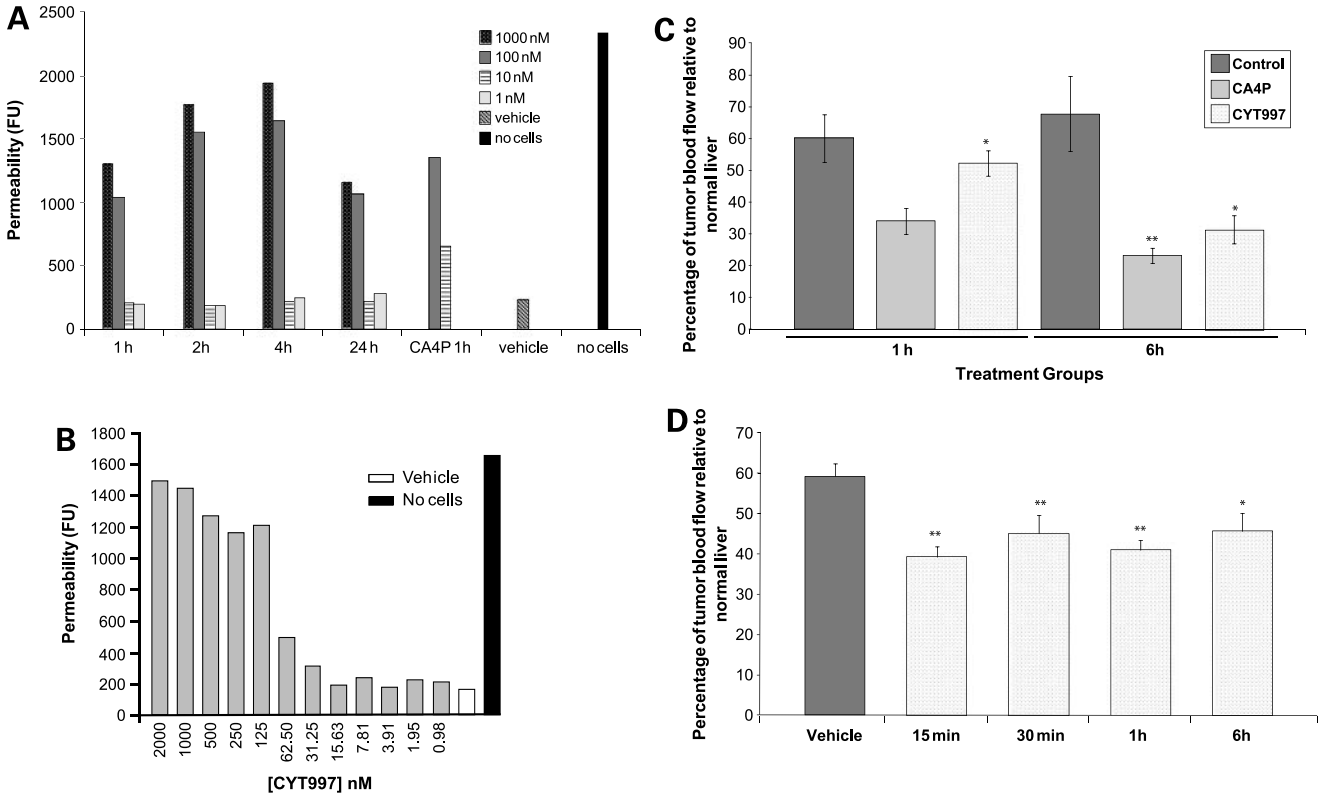

Figure 5. CYT997 possesses antivascular activity. **A,** CYT997 increases the permeability of the HUVEC monolayer. Time course measurement of HUVEC monolayer permeability after exposure to CYT997 was determined by monitoring permeation of FITC-Dextran through confluent layers of cells on inserts in a transwell configuration. The extent of permeability was determined by measuring the fluorescence of the well solution using a fluorometer. Permeability is expressed in fluorescence units in the receiving well. **B,** dose-response curve for effect of CYT997 on HUVEC monolayer permeability. Permeability was determined as described above and measured after 1 h of drug exposure. **C,** CYT997 decreases tumor blood flow in liver metastases when dosed i.p. The effect of CYT997 (7.5 mg/kg, i.p.) and CA4P (100 mg/kg, i.p.) on tumor blood flow (mean ± SEM) in a mouse model of colorectal liver metastases measured by laser Doppler flowmetry relative to normal liver blood flow. *, $P = 0.01$ versus respective controls; **, $P = 0.001$ versus respective controls. Statistical analysis done using *t* test, two samples assuming unequal variances. **D,** CYT997 decreases tumor blood flow in liver metastases when dosed orally. Effect of CYT997 (20 mg/kg, p.o.) on tumor blood flow (mean ± SEM) in a mouse model of colorectal liver metastases measured by laser Doppler flowmetry relative to normal liver blood flow. *, $P = 0.03$ versus respective control; **, $P = 0.0008$ versus respective control. Statistical analysis done using ANOVA, LSD post hoc analysis.

cell death. In a separate experiment using the lung cancer cell line A549, an accumulation of cyclin B1 was observed in cells treated with vinblastine and CYT997, over those exposed to vehicle alone (Fig. 3A). Furthermore, the levels of phosphorylated serine modified Bcl-2 also increased over time, whereas there was no change in total Bcl-2 detected. Accumulation of cyclin B, which plays a key regulatory role in mitosis, is consistent with G_2-M arrest, as is phosphorylation of Bcl-2 (19, 20). Activation of the proapoptotic enzyme caspase-3 in the cells of hormone-refractory prostate cancer cell line PC3 treated with CYT997 is shown in Fig. 3B. Caspase-3 activation, the last phase in the apoptotic caspase pathway, clearly showed a time-dependent increase for CYT997-treated cells. Cleavage of the caspase-3 substrate PARP was observed over a similar time frame in A549 cells treated with CYT997 (Fig. 3C). In addition, apoptosis was also measured in A549 cells exposed to either CYT997 or vinblastine by FACS analysis using Annexin V and propidium iodide as markers of changes and breakdown of the cellular membrane that occur during apoptosis. Cells positive for both Annexin V and propidium iodide are in the late stages of apoptosis, and a time-dependent increase of Annexin V and propidium iodide–positive cells compared with control is clearly evident in CYT997 and vinblastine-treated cells (Fig. 3D).

CYT997 Is an Orally Bioavailable Inhibitor of Tumor Growth *In vivo*

Given the potent cytotoxic activity of CYT997 and its promising pharmacokinetics and oral bioavailability, we assessed the activity of the compound in two distinct murine cancer models. In a xenograft model using the human prostate cancer cell line PC3, oral dosing of CYT997 was initiated 13 days after cell implantation by which time palpable tumors were evident. A dose-dependent inhibition of tumor growth was apparent with CYT997, which at the highest dose was equivalent to parenterally administered paclitaxel (Fig. 4A). The initial high dose cohort of CYT997 (30 mg/kg/d), however, showed signs of cachexia in some mice and the dose was decreased to a 25 mg/kg/d, which was well tolerated.

Excellent activity was also observed for orally dosed CYT997 in an orthotopic syngeneic model using the mouse breast cancer cell line 4T1, with activity similar to the positive control platinol for the high-dose cohort (Fig. 4B). Paclitaxel, in contrast, showed limited activity, similar to lower doses of CYT997, against this aggressive tumor type. In a separate experiment, variation of dosing schedule also showed promising antitumor activity. Thus, twice weekly dosing of CYT997 at 80 mg/kg p.o. showed similar efficacy to thrice weekly dosing at 70 mg/kg, and daily dosing at 30 mg/kg, indicating that flexibility in dosing regimens should be efficacious in a clinical setting (Fig. 4C).

CYT997 Exhibits Antivascular Activity *In vitro* and *In vivo*

Most microtubule binding agents are now recognized to possess some degree of vascular-disrupting activity (21), and therefore, the antivascular effects of CYT997 were assessed in two separate models. Thus, the permeability barrier function of endothelial cells was evaluated using an *in vitro* model in which a confluent monolayer of HUVECs was exposed to CYT997 and the extent of permeation of FITC-Dextran across the monolayer was determined. As shown in Fig. 5A, CYT997 caused a rapid increase in the permeability of HUVEC monolayers and the increase in permeability was detectable as early as 1 hour after the addition of the compound. The effect reached a maximum after 4 hours of exposure and persisted up to 24 hours. This effect was reversible after compound washout and 24-hour recovery, with HUVEC monolayers recovering their barrier function and the permeation of freshly added FITC-Dextran being prevented (data not shown). The IC_{50} of CYT997 increase in permeability of HUVEC monolayers was estimated to be ~80 nmol/L at 1 hour of exposure (Fig. 5B).

The vascular disrupting effects of CYT997 were studied *in vivo* using pulsed laser Doppler flowmetry, a technique that has been used previously to measure blood flow in metastatic tumors (17). In this work, blood flow was measured in individual tumors on the liver surface of anesthetized mice 1 or 6 hours after CYT997 or vehicle administration, and compared directly to CA4P-treated animals as a positive control. A single dose of CYT997 (7.5 mg/kg i.p.) clearly decreased blood flow in liver metastases, and a significant reduction in blood flow was present 6 hours postdose (Fig. 5C), similar to the positive control CA4P (100 mg/kg, i.p.). When CYT997 was dosed orally, blood flow was significantly reduced at 15 minutes, and remained suppressed at 6 hours (Fig. 5D).

Discussion

Microtubules are highly dynamic structures responsible for the establishment and maintenance of cell shape, and for the organization of the mitotic spindle along which the metaphase chromosomes assemble prior to mitosis. Disruption of microtubule dynamics through the binding of drugs to tubulin subunits therefore affects these multiple functions of microtubules and leads to the cytotoxic effects of several approved drugs such as the taxanes, paclitaxel and docetaxel, and the *Vinca* alkaloids, vincristine, vinblastine, and vinflunine. In an effort to discover drugs with improved pharmaceutical and physicochemical properties to these conventional agents, much research has been conducted in recent years in the identification and study of small molecule compounds that bind to tubulin and disrupt microtubule dynamics (8).

This work describes CYT997, a novel synthetic small molecule optimized for antiproliferative activity in a panel of cell-based assays, in which the compound shows an IC_{50} of between 1 and 100 nmol/L across a panel of cancer cell lines. The compound inhibits the polymerization of tubulin with an IC_{50} of ~3 μmol/L, which is similar to the inhibitory activity of other small molecule microtubule poisons (3). Confocal microscopy clearly shows that the microtubule network in cells is rapidly destroyed, and if left in the presence of the drug, cells lose their normal distribution of tubulin along with their typical morphology. Washout of the drug after a 1-hour exposure, however, allows the cells to fully recover, indicating that the effect on microtubules is reversible in this time frame.

Disruption of microtubule dynamics causes blockade of the transition of cells from the G_2 phase into mitosis through the disruption of the establishment of a functional mitotic spindle (22). CYT997 causes a significant increase of cells in the G_2-M phase of the cell cycle, as determined by FACS analysis. In addition, Western blot analysis of cyclin B1 expression levels in A549 cells indicated that CYT997 and vinblastine-treated cells show an upregulation of cyclin B1 compared with control cells. Cyclin B1 plays a key regulatory role during mitosis, and increased levels of this protein have been observed in cells treated with other microtubule poisons such as paclitaxel (23). Similarly, phosphorylation of Bcl-2, which is considered a marker of mitotic arrest, was also observed in CYT997 and vinblastine-treated cells, mirroring results reported for other microtubule targeting agents (24, 25).

The involvement of members of the Bcl-2 family of proteins in the regulation of apoptosis is well documented, with the loss of Bcl-2 activity being associated with an induction of the activities of a number of proteases, such as members of the caspase family, and other enzymes such as PARP. Furthermore, numerous studies have shown that caspases are key participants in the sequence of events leading to apoptosis, and that activation of caspase-3 is a hallmark of cellular commitment to apoptosis (26). The effects of CYT997 on the apoptotic pathway were investigated by examination of the induction of activated caspase-3 and PARP, and Fig. 3B clearly shows that caspase-3 is activated in PC-3 cells treated with CYT997 being apparent from 6 hours. Activation of caspase-3 is also evident in A549 cells treated with CYT997 following the appearance of a large fragment of human PARP, which arises through caspase-3–mediated cleavage of PARP1, an enzyme involved in DNA repair (Fig. 3C). Changes to the surface lipid bilayer composition, in particular, translocation of phosphatidylserine from the inner membrane leaflet to the outer, are an early consequence of the induction of apoptosis in cells.

The Annexin V protein binds with high affinity to phosphatidylserine lipids, and quantitation of this binding allows the measurement of apoptotic cells. In addition, disruption of cellular membrane integrity, a latter marker of apoptosis, could be quantitated by propidium iodide nuclear staining. In normal cells, propidium iodide is impermeant; however, breakdown of membrane bilayer integrity allows propidium iodide to penetrate the cell and bind to DNA. Figure 3D clearly depicts that CYT997 treatment of A549 cells causes a time-dependent increase in Annexin V and propidium iodide–positive cells, and furthermore, in a similar time frame and with a similar magnitude to cells treated with vinblastine. Taken together with FACS data on the cell cycle, the molecular analysis of the pathways affected suggests that CYT997 first blocks the passage of cells through the cell cycle at the G_2-M boundary, and then drives the cells towards death through apoptotic pathways.

In addition to its microtubule inhibitory and cytotoxic activity, CYT997 has attractive pharmaceutical properties and oral bioavailability, and has shown efficacy in animal models when administered orally. Thus, significant antitumor activity has been shown in a prostate cancer xenograft model and in a breast cancer syngraft model using orally dosed CYT997. Importantly, good activity is realized with only twice weekly dosing of the compound. By contrast, many microtubule targeting agents show limited oral activity and often require intravenous administration.

The disruptive effect that many microtubule targeting drugs have on tumor vasculature has been realized in recent years (21, 27), and we therefore sought to determine whether CYT997 possessed similar properties. In an *in vitro* model of endothelium integrity, CYT997 caused significant time-dependent and dose-dependent disruption to a confluent monolayer of HUVEC cells, as measured by permeation of FITC-labeled dextran across the monolayer, with potency slightly weaker than the known vascular disrupting agent, CA4P. *In vivo*, the effect of CYT997 on tumor blood flow was monitored using pulsed laser Doppler flowmetry on metastatic tumors located on the surface of livers of anesthetized mice. In this study, a single dose of CYT997 (7.5 mg/kg, i.p.) reduced tumor blood flow significantly at 6 hours. Notably, a low dose of CYT997 suppressed tumor blood flow to a similar extent as the positive control CA4P dosed at 100 mg/kg. When dosed orally (20 mg/kg), the effect on tumor blood flow was not as great as observed by i.p. administration, however, the effect was greatest at the earlier time point of 15 minutes and slowly decreased over 6 hours, although the reduction in flow was still significant compared with control. The more rapid onset seen in the orally dosed animals most likely arises through higher drug concentration in the liver on absorption of the oral dose. The antitumor effect of CYT997 observed in the xenograft and syngraft models discussed above is most likely a result of a combination of tumor vascular disruption and direct cytotoxic activity against the tumor cell line, and studies to further delineate these effects are ongoing.

The introduction of a well-tolerated orally active inhibitor of microtubule dynamics would provide a significant improvement in the range of treatment options for patients with cancer. We believe that the development of CYT997 will lead to new and important treatment regimens, providing both bolus dosing options as well as the possibility of consistently maintaining lower plasma levels through oral dosing regimens. CYT997 is currently undergoing clinical trials with both i.v. and p.o. administration in a variety of cancer indications, and phase I data from both presentations of the drug have recently been reported (28, 29). The results of these early clinical studies and the preclinical data reported herein support the continuing evaluation of this novel drug.

Disclosure of Potential Conflicts of Interest

C.J. Burns, E. Fantino, I.D. Phillips, S. Su, M.F. Harte, P.E. Bukczynska, M. Frazzetto, M. Joffe, I. Kruszelnicki, B. Wang, Y. Wang, N. Wilson, S.S. Wan, R. Fida, and A.F. Wilks are former or current employees of Cytopia. Some of the above are also equity holders in Cytopia.

Acknowledgments

Mouse xenograft studies were performed at Vivopharm Pty., Ltd., Adelaide, Australia with helpful advice from Dr. Ralf Brandt. Drs. Gregg Smith and David Segal are thanked for review of the manuscript as is Valentina Dublevic for technical assistance.

References

1. Wood KW, Cornwell WD, Jackson JR. Past and future of the mitotic spindle as an oncology target. Curr Opin Pharmacol 2001;1:370–7.

2. Jordan MA, Wilson L. Microtubules as a target for anticancer drugs. Nat Rev Cancer 2004;4:253–65.

3. Jordan A, Hadfield JA, Lawrence NJ, McGown AT. Tubulin as a target for anticancer drugs: agents which interact with the mitotic spindle. Med Res Rev 1998;18:259–96.

4. Honore S, Pasquier E, Braguer D. Understanding microtubule dynamics for improved cancer therapy. Cell Mol Life Sci 2005;62:3039–56.

5. Mollinedo F, Gajate C. Microtubules, microtubule-interfering agents and apoptosis. Apoptosis 2003;8:413–50.

6. Orr GA, Verdier-Pinard P, McDaid H, Horwitz SB. Mechanisms of Taxol resistance related to microtubules. Oncogene 2003;22:7280–95.

7. Gelderblom H, Verweij J, Nooter K, Sparreboom A. Cremophor EL: the drawbacks and advantages of vehicle selection for drug formulation. Eur J Cancer 2001;37:1590–98.

8. Kuppens IELM. Current state of the art of new tubulin inhibitors in the clinic. Curr Clin Pharmacol 2006;1:57–70.

9. Carlson RO. New tubulin targeting agents currently in clinical development. Expert Opin Investig Drugs 2008;17:707–22.

10. Ferlini C, Gallo D, Scambia G. New taxanes in development. Expert Opin Investig Drugs 2008;17:335–47.

11. Orosz F, Comin B, Raïs B, et al. New semisynthetic *Vinca* alkaloids: chemical, biochemical and cellular studies. Br J Cancer 1999; 79:1356–65.

12. Altaha R, Fojo T, Reed E, Abraham J. Epothilones: a novel class of non-taxane microtubule-stabilizing agents. Curr Pharm Des 2002;8: 1707–12.

13. Tozer GM, Kanthou C, Baguley BC. Disrupting tumour blood vessels. Nat Rev Cancer 2005;5:423–35.

14. Burns CJ, Harte MF, Bu X, et al. Discovery of CYT997: a structurally novel orally active microtubule targeting agent. Bioorg Med Chem Lett 2009;19:4639–42.

15. Schwaller J, Frantsve J, Aster J, et al. Transformation of hematopoietic cell lines to growth factor independence and induction of a fatal myelo- and lympoproliferative disease in mice by retrovirally transduced Tel/JAK2 fusion genes. EMBO J 1998;17:5321–33.

16. Peeters P, Raynaud SD, Cools J, et al. Fusion of TEL, the ETS-variant gene 6 (ETV6), to the receptor-associated kinase JAK2 as a result of

t(9;12) in a lymphoid and t(9;15;12) in a myeloid leukemia. Blood 1997; 90:2535–40.

17. Kuruppu D, Christophi C, Bertram JF, O'Brien PE. Characterization of an animal model of hepatic metastasis. Gastroenterol Hepatol 1996;11: 26–32.

18. Loganzo F, Discafani CM, Annable T, et al. HTI-286, a synthetic analogue of the tripeptide hemiasterlin, is a potent antimicrotubule agent that circumvents P-glycoprotein-mediated resistance *in vitro* and *in vivo*. Cancer Res 2003;63:1838–45.

19. Thornton BR, Toczyski DP. Securin and B-cyclin/CDK are the only essential targets of the APC. Nat Cell Biol 2003;5:1090–4.

20. Haldar S, Basu A, Croce CM. Bcl2 is the guardian of microtubule integrity. Cancer Res 1997;57:229–33.

21. Schwartz EL. Antivascular actions of microtubule-binding drugs. Clin Cancer Res 2009;15:2594–601.

22. Wassmann K, Benezra R. Mitotic checkpoints: from yeast to cancer. Curr Opin Genet Dev 2001;11:83–90.

23. Mulligan JM, Greene LM, Cloonan S, et al. Identification of tubulin as the molecular target of proapoptotic pyrrolo-1,5-benzoxazepines. Mol Pharmacol 2006;70:60–70.

24. Tinley TL, Randall-Hlubek DA, Leal RM, et al. Taccalonolides E and A: plant-derived steroids with microtubule-stabilizing activity. Cancer Res 2003;63:3211–20.

25. Basu A, Haldar S. Microtubule-damaging drugs triggered bcl2 phosphorylation-requirement of phosphorylation on both serine-70 and serine-87 residues of bcl2 protein. Int J Oncol 1998;13:659–64.

26. Earnshaw WC, Martins LM, Kaufmann SH. Mammalian caspases: structure, activation, substrates, and functions during apoptosis. Annu Rev Biochem 1999;68:383–424.

27. Kanthou C, Tozer GM. Tumour targeting by microtubule-depolymerising vascular disrupting agents. Expert Opin Ther Targets 2007;11: 1443–57.

28. Lickliter J, Smith G, Burge M, et al. Phase I study of CYT997, a novel cytotoxic and vascular disrupting agent, given as a 24-hour intravenous infusion to patients with advanced solid tumours. J Clin Oncol 2007; 25:14115.

29. Francesconi A, Kotasek D, Burge M, Smith G, Lickliter J. Phase I evaluation of orally-administered CYT997, a novel cytotoxic vascular-disrupting agent, in patients with advanced cancer. J Clin Oncol 2009;27:3568.